FEATURE ARTICLE

Laser Spectroscopy of Jet-Cooled Biomolecules and Their Water-Containing Clusters: Water Bridges and Molecular Conformation

Timothy S. Zwier

Department of Chemistry, Purdue University, West Lafayette, Indiana 47907-1393

Received: May 2, 2001; In Final Form: July 6, 2001

The techniques of laser-induced fluorescence (LIF), resonant two-photon ionization spectroscopy (R2PI), UV−UV hole-burning spectroscopy, fluorescence-dip infrared spectroscopy (FDIRS), and resonant ion-dip infrared spectroscopy (RIDIRS) have been used to study the ultraviolet and infrared spectra of individual conformations of small, flexible biomolecules cooled in a supersonic expansion. The water-containing clusters of these molecules and of other rigid molecules that possess multiple H-bonding sites are considered. The water molecules in many of the solute−$(water)_n$ clusters form hydrogen-bonded bridges between donor and acceptor sites on the solute molecule. The infrared spectroscopy of these bridges has been explored in some detail. Water bridges are also formed when one of the H-bonding sites is on a flexible side chain. These bridges have a profound influence on the conformational preferences of the flexible biomolecules.

I. Introduction

One of the keys to understanding a molecule's behavior is to know its shape. As physical chemists, we typically look to spectroscopy to answer such questions. However, many molecules, when interrogated for their structure, give no single answer. The molecules are flexible, with population spread over more than one conformational minimum, between which they transform on time scales that are governed by the unique corrugation of their potential energy surfaces.

When such a flexible molecule is placed in solution, its conformational preferences often change, sometimes in startling ways. While aspects of these changes can be accounted for by dielectric continuum models,[1] individual solvent molecules in the first solvent shell also can play a unique and important role, especially in hydrogen bonding solvents such as water.[2,3] The influence of such "bound water" on the conformational preferences of flexible biomolecules is difficult to study by optical spectroscopy in solution because it is not easy to assign infrared or ultraviolet absorptions to individual conformations, and even more difficult to distinguish the water molecules bound to the solute in the presence of a huge excess of water molecules in the bulk.

One of the intriguing solvation structures sometimes implicated by condensed phase studies is the hydrogen-bonded bridge.[4,5] When a solute molecule possesses both hydrogen bond donor and acceptor sites, a chain of donor−acceptor water molecules can sometimes effectively "bridge the gap" between these sites. Such bridges, once formed, gain stability from the cooperative strengthening of the hydrogen bonds in the bridge. To form the water bridge, the flexible molecule may need to bend in ways that are not favorable in the absence of the solvent bridge. These are the molecular-scale solvation effects one would like to probe and understand. Furthermore, the role of water bridges as "proton conduits" between proton donor and acceptor sites is thought to be important in solution,[6−8] though difficult to prove.

This article is an account of recent studies by our group of the infrared and electronic spectroscopy of supersonically cooled, isolated biomolecules and their clusters with water in the gas phase. Such studies offer a unique vantage point for viewing the spectroscopic consequences induced by a molecule changing its conformation. It also enables the study of the effects of water molecule(s) binding to and between particular sites on a molecule, whether singly or in hydrogen bonded networks.

II. Conformational Cooling and Cluster Formation in a Supersonic Expansion

By seeding the "solute" molecules in a supersonic expansion,[9] the molecules are collisionally cooled to very low effective temperatures, thereby removing vibrational hot bands and collapsing the rotational population into levels commensurate with a rotational temperature of about 5 K. This reduces the congestion and complexity of an optical spectrum, greatly aiding the assignment of the observed transitions. When the solute molecule is conformationally flexible, the supersonic cooling typically quenches the population into the zero-point levels of each of the individual conformations if the barriers separating them are sufficiently high. For example, as Figure 1 shows, the low-lying conformational isomers of tryptamine (TRA) are on a two-dimensional potential energy surface involving internal rotation about two "flexible" bonds in the ethylamine side chain: the C(α)−C(*β*) bond that establishes the amino group's *position* and the C(α)−amino N bond that establishes the amino group's *orientation*.[10,11] The 3-fold barriers that accompany internal rotation about either of these axes give rise to nine low-lying conformational minima in tryptamine, seven of which have energies that are thermally accessible at the preexpansion temperature.[11] As we shall see, the ultraviolet spectrum of jet-

10.1021/jp011659+ CCC: $20.00
Published on Web 08/25/2001

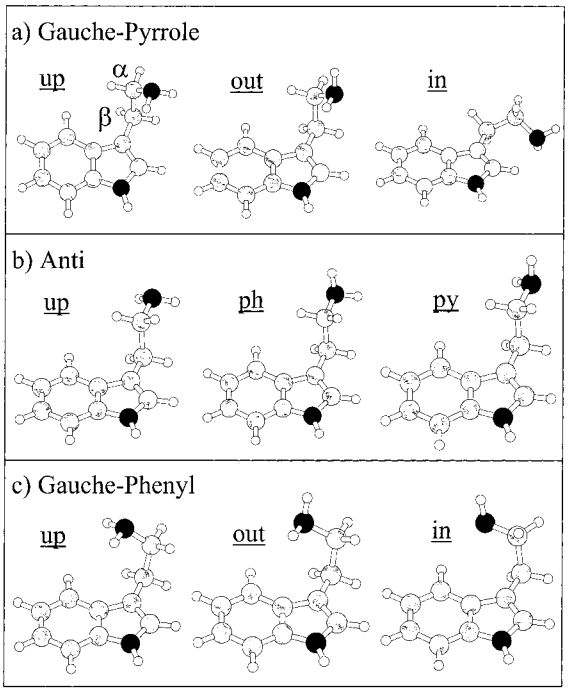

Figure 1. Calculated structures of the nine lowest-energy minima of the tryptamine monomer. The nine minima lie nominally on a two-dimensional potential energy surface involving internal rotation about the C(α)−C(*β*) and C(α)−N bonds. The Gpy(in) and Gph(in) structures are significantly higher in energy than the other seven and are not observed experimentally.

cooled tryptamine has an S_1-S_0 origin region with seven origins due to seven conformers, just as the energetics would suggest.

Thus, while the tryptamine molecules are rotationally and vibrationally cold, their conformational distribution is not necessarily so.[11,12] Thus, spectroscopic studies of supersonically cooled, flexible molecules have the potential for providing resolved, assignable vibrational and electronic spectra due to the individual conformations of those molecules with significant population in the preexpansion gas mixture. These can be studied in the expansion free from interference from solvent or matrix effects.

The supersonic expansion also can act as a synthetic tool for making molecular clusters.[9] Introduction of solvent vapor (e.g., water) into the expansion along with the solute of interest produces solute−(solvent)$_n$ clusters whose size distribution is determined by the relative concentrations and absolute pressure of the supersonic expansion. In a molecule with multiple H-bonding sites, one wishes to know which binding site is preferred by the first water molecule. For instance, the amino group in tryptamine (Figure 1) can accept a hydrogen bond from water, while the indole NH group can donate a hydrogen bond to water. The question is whether one is favored over the other in the supersonic expansion, and to what extent.

On the basis of the trapping of population in local minima observed for the flexible monomers, one might anticipate a similar trapping to occur in cluster formation. However, a growing body of evidence suggests that in water-containing clusters, two-body displacement collisions often funnel the clusters toward the most stable structures with high efficiency.[13] As we shall see in tryptamine, for instance, the first water preferentially binds at the amino group on the ethylamine side chain,[14] with only the smallest hint of any population in the indole NH-bound complex.[15] This is consistent with the expected stronger binding at the amino site.

Regardless of the mechanism, this means that the clusters formed in a supersonic expansion are typically those with the most stable "solvation" structures. One hopes, then, to study these most stable solvation structures as a function of the number of water molecules in the cluster, where solute−solute, solute−solvent, and solvent−solvent interactions contribute to the total stability of the cluster. We will see that in these larger solute−(water)$_n$ clusters, water bridges often form between H-bonding sites on the solute. The study of these water-containing clusters then provides spectroscopic signatures for the H-bonded bridges. Furthermore, when water binds to a solute molecule with conformational flexibility, one can begin to ask questions about the influence of water binding on the conformational preferences of the flexible molecule. We will see that bridge formation can dramatically alter the conformational preferences of a flexible solute.

III. Experimental and Theoretical Methods

A necessary first step in addressing any of the issues just posed is to disentangle the spectra due to the various conformers and molecular clusters in the expansion. This challenge has produced many creative and powerful solutions from the spectroscopy community.[13,16−28] We focus here on a collection of methods that are particularly well suited to the study of large aromatic molecules and their water-containing clusters.[13,27−32] As we shall see, many of the aromatic molecules of interest have particular biological relevance that motivate their study. From a practical standpoint, however, their strong ultraviolet absorptions facilitate their sensitive detection via either laser-induced fluorescence (LIF)[33] or resonance-enhanced two-photon ionization (R2PI).[34−37] When the aromatics have flexible side chains, the weak interactions of these side chains with the aromatic ring lead to shifts in the S_1-S_0 spectrum that are often sufficient to separate the transitions of one conformer from another, at least in favorable cases. Coupling R2PI with time-of-flight mass analysis of the ions provides both mass and wavelength discrimination of the species present in the expansion. This is particularly important in the studies of solute−(water)$_n$ clusters as a function of cluster size.

Even with mass analysis, however, there is often more than one species contributing to the signal in a given mass channel (e.g., the various conformational isomers of the monomer), requiring another level of dissection of the observed R2PI spectra. UV−UV hole-burning (Figure 2) can be used to identify all the vibronic transitions due to a single species in the R2PI spectrum. Hole-burning spectra can be recorded either by tuning the hole-burn or probe laser. In the present examples, we do the latter. The UV laser that is used as a hole-burning source is fixed on a particular transition that it partially saturates. The hole-burning spectrum is then recorded by tuning a time-delayed, probe UV source through the R2PI spectrum while monitoring the difference in ion or fluorescence intensity with and without the hole-burning laser present. All vibronic transitions that arise from the same ground-state level probed by the hole-burning laser show up as depletions in the hole-burning spectrum, effectively providing the UV spectrum of each species present in a given mass channel, free from interference from the others. The fluorescence-based analogue of this experiment can also be carried out, giving up mass selectivity for experimental convenience or signal size.

Whether it is conformational isomers or water-containing clusters that are of interest, the frequencies and intensities of the low-frequency vibronic transitions in the ultraviolet spectrum can be used to assign structures and probe their interactions.[38]

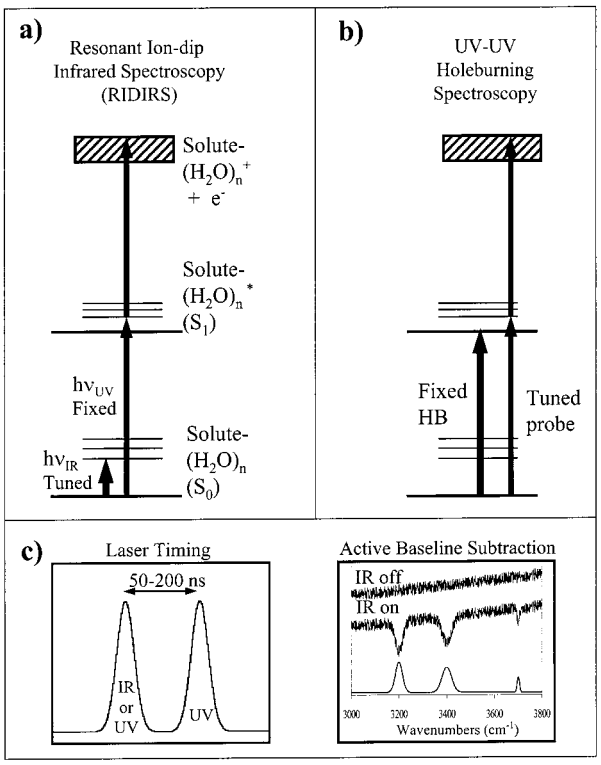

Figure 2. Schematic energy level diagrams for (a) resonant ion-dip infrared spectroscopy (RIDIRS) and (b) UV−UV hole-burning spectroscopy. (c) Timing diagram for the two methods, in which the depletion or hole-burning laser precedes the UV probe laser by 50−200 ns. (d) Pictorial representation of active baseline subtraction, applied here to the RIDIR method. The IR source is pulsed every other time the ultraviolet source fires, and the difference in ion signal between the two is recorded as a function of infrared wavelength.

This low-frequency region of the spectrum is particularly ripe with information about the cluster, since much of the observed structure involves intermolecular vibrations. At the same time, without rotational resolution, assignment of the monomer conformation or water cluster topology based on the vibronic level data provided by the LIF or R2PI spectrum can be difficult, especially as the size of the cluster grows. Furthermore, in the study of solute−$(solvent)_n$ clusters, the solvent molecules are not involved directly in the electronic transition, and are thus viewed only indirectly by the perturbations they impose on the solute molecule's electronic spectrum.

The infrared spectrum in the hydride stretch region (2800−3800 cm^{-1}) provides a more direct probe of the hydrogen bonding topology of the flexible monomers and water-containing clusters. When an XH group (where X, Y are electronegative atoms) is placed in a hydrogen bond XH···Y, the XH stretch fundamental responds by shifting down in frequency (often by hundreds of wavenumbers), increasing its intensity (often by a factor of 10 or more), and increasing its width.[39] This makes the XH stretch fundamentals particularly sensitive signatures of the number, type, and strength of the hydrogen bonds present, including those of water.[13] The appearance of the spectrum is also affected by the magnitude of the coupling between the XH groups and the degree of cooperative strengthening present in the hydrogen-bonded network.

To record the infrared spectrum of a single conformer or cluster, the mass and wavelength selectivity offered by R2PI is used as part of a double resonance technique, which we refer to as resonant ion-dip infrared spectroscopy (RIDIRS).[13] A schematic diagram for the method is shown in Figure 2. The

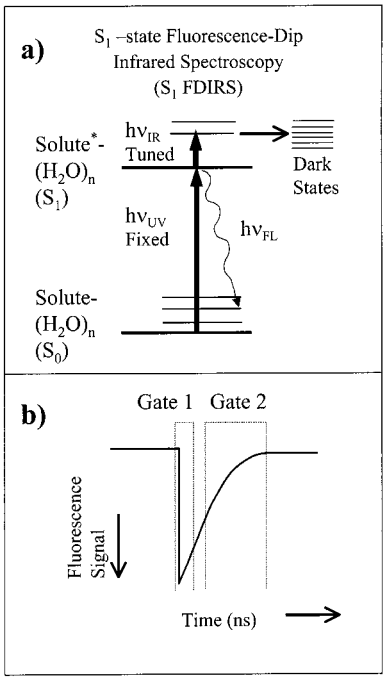

Figure 3. Schematic diagram of (a) the S_1-state fluorescence-dip infrared technique and (b) the fluorescence-normalization procedure. The infrared laser promotes the excited-state population to vibrationally excited levels that have fast nonradiative processes, thereby quenching the fluorescence. Gate 1 and Gate 2 refer to the gated portion of the fluorescence signal corresponding to firing of the UV and IR lasers, respectively.

RIDIRS technique has its genesis in early experiments on benzene by Page et al.,[40,41] and is currently used with minor variation by many groups worldwide.[13,27−31] In our case, the infrared output is provided by a seeded Nd:YAG-pumped KTA-based optical parametric converter. This infrared source operates at half the frequency of the ultraviolet laser(s) used for R2PI, with which it is spatially overlapped. The UV source is then fixed to a desired vibronic transition in the R2PI spectrum, creating a constant ion signal in the particular mass channel of interest in the time-of-flight mass spectrum. The IR source is scanned through the desired wavelength region of interest (typically 2800−3800 cm^{-1}). When an infrared transition of the selected conformer or cluster is encountered, its ground-state population, and thus the constant ion signal, is depleted. The difference between the ion signal with and without the IR present is then monitored via active baseline subtraction methods.

As with the hole-burning methods, there is a fluorescence-based analogue of the RIDIRS experiment; namely, fluorescence-dip infrared spectroscopy (FDIRS), that has been used in several cases where fluorescence detection is preferred. Furthermore, the FDIRS method can be easily extended to record the hydride stretch infrared spectra of different vibronic levels in the S_1-state.[27,42] Most of what we know about the vibrations in electronically excited states comes from vibrationally resolved electronic spectroscopy. In large molecules, vibrational congestion, poor Franck−Condon factors, and decreasing fluorescence quantum yields typically limits assignments of vibronic structure to the region within 1500 cm^{-1} of the S_1 origin. Thus, comparatively little is known about the S_1-state hydride stretch vibrations of these molecules and their clusters. Several years ago, Huber and co-workers[42] demonstrated the S_1-state analogue of fluorescence-dip infrared spectroscopy (FDIRS) on propynal. As shown in Figure 3a), in S_1-state FDIRS, the timing between

UV and IR pulses is changed from that used for ground-state FDIRS simply by delaying the IR so that it occurs *after* rather than *before* ultraviolet excitation. If the infrared excitation occurs while population remains in the S_1-state, it promotes population out of the fluorescing S_1 level to vibrationally excited levels in S_1 with much smaller fluorescence quantum yields, resulting in a depletion in the tail of the fluorescence decay signal (Figure 3b). By gating the fluorescence detection on this trailing component of the fluorescence signal, an S_1-state FDIR spectrum can be obtained. A necessary prerequisite for the method of S_1-state FDIR spectroscopy is that the light sources used for the electronic excitation and infrared probe steps be short-lived by comparison to the S_1 excited-state lifetime, so that population can be promoted to the S_1-state and probed prior to loss of the population from the S_1-state.

The experimental methods just described can be used to obtain the infrared and ultraviolet spectra of single conformations of flexible aromatic molecules and of size-selected water-containing clusters. To assign the observed spectra to the correct structures, it is necessary to compare them to calculated spectra of plausible structures. It is only recently that reliable calculations on molecules and clusters of this size have become possible.[43,44] This confluence of progress in experiment and theory is responsible for the recent explosion of interest in such studies. In the work described here, density functional theory (DFT) calculations employing the Becke3LYP functional, typically with a 6-31+G* basis set, have been used as the primary point of comparison with experiment.

IV. Spectroscopy of Single Conformations of Flexible Biomolecules

Tryptamine (TRA) and 3-indole-propionic acid (IPA) are close analogues of the aromatic amino acid tryptophan, differing from it by removal of the COOH group (TRA) or NH_2 group (IPA). All low-lying isomers of both molecules share an out-*of*-plane configuration for the ethylamine or propionic acid side chain relative to the indole ring (see Figure 1). As a result, both

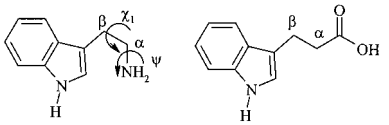

Tryptamine (TRA) 3-indole-propionic acid (IPA)

molecules effectively have only two flexible degrees of freedom involving hindered rotation about the C(α)−C(*β*) and C(α)−X bonds (X = NH_2 or COOH). These determine the *position* and *orientation* of the amino or carboxylic acid groups, respectively. Tryptamine and 3-indole-propionic acid thus represent a manageable starting point for studying the ultraviolet and infrared spectral signatures of single conformations of flexible biomolecules, and were among the first flexible aromatics to be studied in a supersonic jet.[19,45]

Tryptamine has already been used in section II to illustrate the effects of expansion cooling on molecules with conformational flexibility. Figure 4a,b) show the one-color R2PI spectra of TRA and IPA, respectively, in the region of the $S_1 \leftarrow S_0$ origin.[10,11] UV−UV hole burning spectroscopy has been used to confirm that there are seven distinct conformational isomers of TRA present in the expansion, but only two of IPA. The spectroscopy of both molecules has been studied by several groups, [14,19,46,47] culminating in a complete conformational assignment for each, based in part on conformation-specific infrared spectra.[10,11] The labeling scheme used to designate the

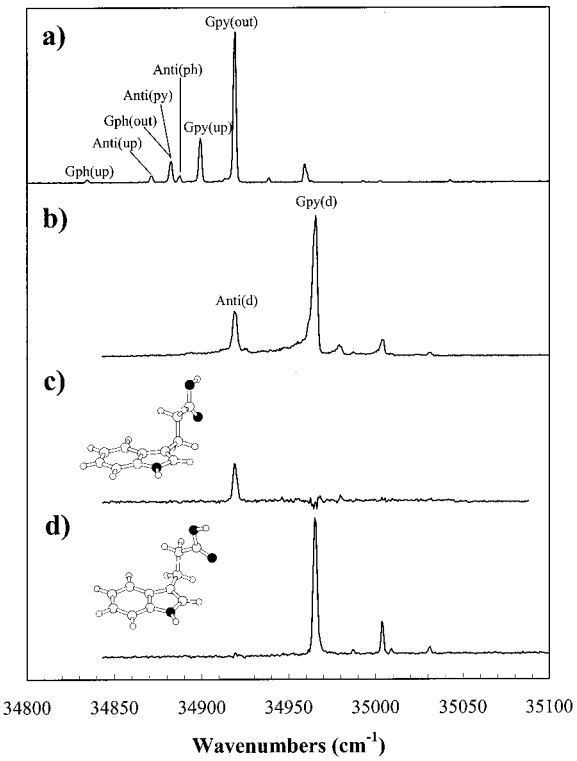

Figure 4. One-color R2PI spectra of (a) tryptamine (TRA), and (b) 3-indole-propionic acid (IPA) in the S_1-S_0 origin region. (c and d): UV−UV hole-burning spectra of the (c) anti(d) and (d) Gpy(d) conformers of IPA.

conformers denotes the position of the amino or carboxylic acid group relative to the indole ring, whether gauche on the phenyl side of indole (Gph), gauche on the pyrrole side of indole (Gpy), or anti. The orientation of the amino group lone pair or carbonyl group relative to the indole ring is given in parentheses (up, out, down, side). UV−UV hole-burning is used in Figure 4c,d) to dissect the R2PI spectrum of IPA into its constituent parts due to anti(down) and Gpy(down), respectively.

Figure 5 shows the RIDIR spectra of the most stable conformations of TRA (Gpy(out)) and IPA (Gpy(down)), taken by monitoring the ion signal at the $S_1 \leftarrow S_0$ origins of these conformations in the R2PI spectra of the two molecules (Figure 4).[10,11] The RIDIR spectra neatly divide into hydride stretch fundamentals due to different XH groups in the molecules, whether indole NH, amino NH, carboxylic acid OH, aromatic CH, or alkyl CH in kind. The corresponding spectra of the other conformations (not shown) show similar spectral patterns. Not surprisingly, it is the alkyl CH stretch modes associated with the flexible alkyl side chain that are perturbed most profoundly by the conformational changes, while other hydride stretch groups remote from these sites (e.g., indole NH) are hardly affected. The comparison between experiment and calculation has led to the conclusion that it is the orientation of the NH_2 or COOH group (rather than its position relative to the ring) that plays the major role in determining the appearance of the alkyl CH stretch fundamentals. The infrared spectra of TRA can thus be grouped into a set of three conformers that share the amino "lone-pair up" orientation, and two sets of two due to gauche-(out) and anti(py/ph) structures. This recognition, when combined with the results from rotational coherence measurements of Felker and co-workers[14,47] and rotational band contour studies from the Levy group,[19,46] provided a basis for the assignments shown in Figure 4a. The observed conformers and their relative populations (taken from the R2PI spectra) are qualitatively

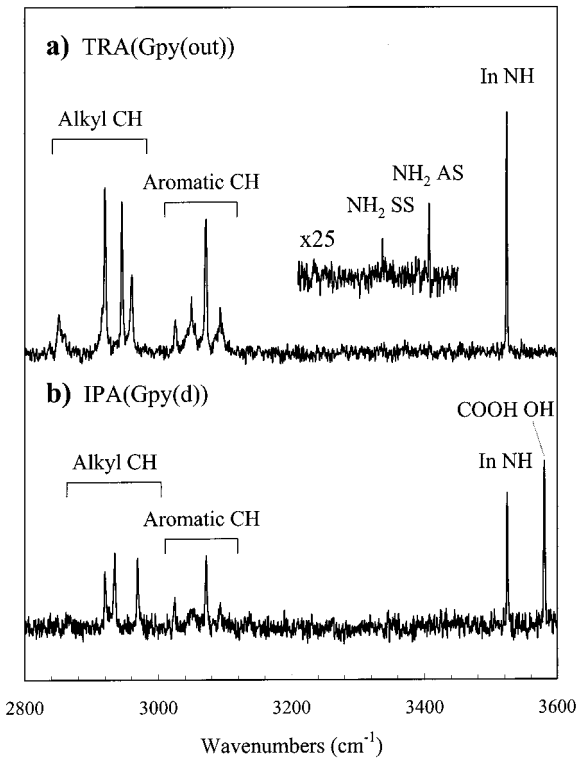

Figure 5. Two examples of RIDIR spectra of single conformations of flexible biomolecules. (A) The Gpy(out) conformer of tryptamine and (b) the Gpy(d) conformer of 3-indole-propionic acid.

consistent with the relative energies of the conformers calculated by the DFT Becke3LYP calculations.

Relaxed potential energy (RPE) scans have been used to gain a firmer understanding of the reasons why there are seven conformers of TRA observed, but only two of IPA.[11] The RPE scans determine the magnitudes of the barriers separating the various conformational minima. In TRA, the 2D potential energy surface for the flexible coordinates contains nine minima (Figure 1) that are separated by large barriers ($\sim$1000 cm^{-1}) relative to kT at the nozzle temperature ($\sim$300 cm^{-1}). Seven of the nine minima are within kT of the global minimum, while the two conformers that point the NH_2 lone pair in toward the indole π cloud are significantly higher in energy than the others. As a result, the pre-nozzle Boltzmann population of TRA contains seven conformers, all of which are cooled with little conformational scrambling into their respective zero-point levels by the expansion.

In IPA, the bulkier COOH group places additional restrictions on the possible conformations of the propionic acid side chain. For instance, the gauche phenyl position for the COOH group is pushed up in energy to the point that the Gph minima will have only small population at 140 °C. In the Gpy or anti positions, the calculations predict that the carbonyl group prefers to point down toward the indole ring, eclipsed with the C(α)−C(β) bond. This leads to two minima, Gpy(down) and anti-(down), which are at least 200 cm^{-1} below all others. These are the two conformers observed experimentally. At the same time, the calculations predict that at least two other minima exist should be thermally populated prior to expansion, yet these are not observed. However, the relaxed potential energy scans identify the reason: these additional minima are very shallow, with barriers small enough ($\sim$100 cm^{-1}) that collisional cooling effectively removes any population from these minima during the expansion.

Simons and co-workers[28,48] have recently carried out an important extension of such conformation-specific studies to the aromatic amino acid phenylalanine. Interestingly, in the amino acid, one need not rely only on the alkyl CH stretch region for the distinction between conformers, because several of the observed conformers possess an intramolecular H-bond between the carboxylic acid OH group and the lone pair on the amino group. When this intramolecular H-bond is present, the RIDIR spectra exhibit an intense, broadened OH stretch fundamental shifted down to 3200−3300 cm^{-1} by the H-bond. We have observed similar effects when an intramolecular H-bond is formed between the NH and C═O groups on adjacent amide moieties in the conformation-specific FDIR spectra of two dipeptide analogues, *N*-acetyl tryptophan amide (NATA) and *N*-acetyl tryptophan methylamide (NATMA).[49] These results suggest that the infrared spectra of single conformations of larger biomolecules can shed considerable light on the intramolecular H-bonds that are anticipated to play such an important role in the conformational preferences of flexible biomolecules in the gas phase.

V. Water-Containing Clusters and Hydrogen-Bonded Bridges

The flexible aromatic molecules considered in section IV have conformations that are distinguished most readily in the infrared if they form *intramolecular* H-bonded bridges between donor and acceptor sites in the molecule. We shall see in this section that the amphoteric nature of water make it an ideal solvent for forming *intermolecular* bridges between H-bonding sites on a molecule, acting simultaneously as both donor and acceptor. Before turning to these hydrogen-bonded bridges, however, it is useful to contrast them with simpler solute−(water)$_n$ clusters in which the solute possesses a single site at which water acts either as donor or acceptor, but not both.

A. Water Binding at a Single H-Bonding Site. Most aromatic molecules with biological relevance have distinct H-bonding sites. When only a single H-bonding site is present, or if one site is energetically much preferred over others, the site serves as a single, well-defined "nucleation point" for attachment of one or more water molecules. Here we focus on the spectroscopic consequences of H-bond formation in simple bimolecular XH···OH_2 or HOH···X complexes.

In indole−(water)$_n$ clusters, the NH group of the pyrrole ring acts as a H-bond donor toward water (Figure 6a inset). The structure of the indole−(water)$_1$ complex has been thoroughly characterized by high-resolution ultraviolet spectroscopy,[50,51] while the binding energy has been determined by threshold R2PI fragmentation measurements.[52] Figure 6a) shows the RIDIR spectrum of the complex in the hydride stretch region.[53,54] The indole NH stretch fundamental is shifted by −89 cm^{-1} from its value in the indole monomer, in response to the hydrogen bond to water. Since the water molecule is a H-bond acceptor, it possesses OH antisymmetric (3747 cm^{-1}) and symmetric stretch (3652 cm^{-1}) fundamentals due to normal modes that are delocalized over the two OH groups, as they are in the water monomer. These appear within a few wavenumbers of their values in the water monomer (3756 and 3657 cm^{-1}, respectively).

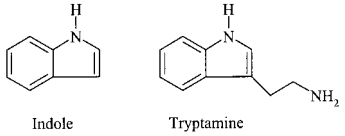

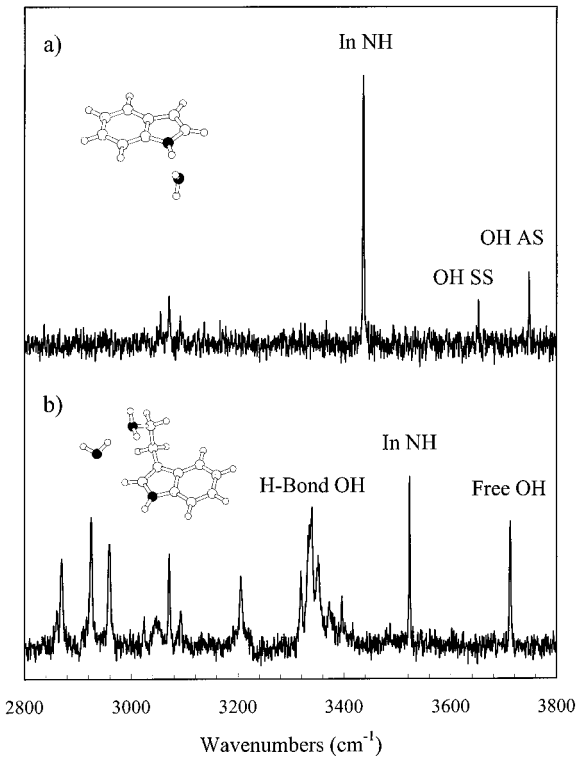

Figure 6. RIDIR spectra of a) the indole$-(H_2O)_1$ complex and (b) the tryptamine$-(H_2O)_1$ complex. The calculated minimum-energy structures for these complexes are shown as insets. These structures are consistent with the experimental spectra.

Tryptamine has two spatially separated H-bonding sites: the indole NH donor site and the NH_2 acceptor site on the flexible ethylamine side chain. Not surprisingly, the amino acceptor site, as a good base, is the energetically preferred binding site for water. Rotational coherence spectroscopy[20] has been used by Connell et al.[14,47] to determine that the tryptamine$-(water)_1$ complex does indeed have the water molecule bound at the amino group, as shown in the inset of Figure 6b). The R2PI spectrum of TRA-H_2O shows a single dominant S_1-S_0 origin transition,[55,56] indicating that complexation of a single water molecule has reduced the number of TRA conformers with significant population from seven to one. The rotational coherence results are consistent with retention of the TRA(Gpy(out)) structure in TRA$-H_2O$ (Figure 6b), and suggest that the stabilization of the water by an indole CH may contribute to the preference for this conformation in the complex.

The RIDIR spectrum of this complex (Figure 6b) shows the characteristic signature of the strong HOH$\cdots$$NH_2$ H-bond that is formed. In forming this H-bond, the normal modes of the water molecule are changed from delocalized antisymmetric and symmetric stretch vibrations to localized vibrations of the H-bonded OH and free OH groups. In the HOH$\cdots$$NH_2$ H-bond, the H-bonded OH stretch fundamental appears as an intense, broadened transition at 3340 cm^{-1}, over 370 cm^{-1} below the frequency of the free OH stretch (3712 cm^{-1}). As the spectrum of Figure 6b) shows, the formation of the H-bond also enhances the intensity of the OH stretch by about a factor of 10 relative to the free OH stretch, as anticipated for a strong H-bond. Finally, the broadening and substructure of the H-bonded OH stretch fundamental is also a common feature of strongly H-bonded XH stretch fundamentals.[39]

In the tropolone-H_2O complex, water binds to the weaker carbonyl acceptor site (HOH$\cdots$O=C) exterior to the intramolecular H-bond of tropolone.[57,58] The H-bonded OH stretch of water appears at 3506 cm^{-1}, shifted by just over 200 cm^{-1} from the free OH stretch. In *trans*-formanilide, the *trans*-amide

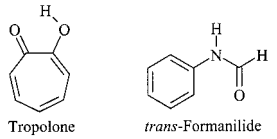

linkage presents both NH donor and C=O acceptor sites, spatially separated from one another. The water-containing clusters of *trans*-formanilide have been studied by several groups.[59−63] The binding energies of these two complexes are nearly identical to one another (5.65 and 5.40 kcal/mol at NH and C=O sites, respectively), and both are observed in the expansion.[62] This interesting circumstance means that the *trans*-amide linkage that is so crucial in polypeptides has two binding sites that can compete with one another for water. When water binds at these two sites, clear infrared spectral signatures are produced. The *trans*-amide NH$\cdots$$OH_2$ complex has an amide NH stretch fundamental shifted -63 cm^{-1} from its monomer value, somewhat less than the shift in the NH stretch of indole$-$water (-89 cm^{-1}). As Mons et al. point out,[62] the smaller shift occurs despite a larger binding energy for the *trans*-amide complex, indicating that care must be taken in correlating the magnitude of the shift with the binding energy if different donor XH groups are involved. The *trans*-amide carbonyl bound water complex has a H-bonded OH stretch fundamental that appears as a doublet at 3513 and 3536 cm^{-1} due to Fermi resonance splitting with the overtone of the carbonyl stretch. These frequencies are close to the value found for tropolone-H_2O (3506 cm^{-1}), consistent with a similar binding at the carbonyl site in the two cases.

B. Hydrogen-Bonded Bridges between Rigid H-bonding Sites. When the solute molecule has both donor and acceptor sites, water can take full advantage of its ability to act both as a H-bond donor and acceptor by forming bridges between these sites of type: D$\cdots$OH$\cdots$OH$\cdots$A.[64−67] Such solvation structures benefit from the cooperative strengthening of the hydrogen bonds in the bridge, much as occurs in forming cyclic water clusters.[68] The pattern of hydride stretch infrared fundamentals due to the bridge XH groups depends sensitively on the nature of the donor and acceptor sites on the solute, the distance between these sites and their relative orientation, the number of water molecules in the bridge, and the magnitude of the coupling between bridge XH groups. The solute donor sites so far considered include indole NH, amide NH, alcohol OH, and carboxylic acid OH groups, while the acceptor sites include amide C=O, carboxylic acid C=O, NH_2, and aromatic π sites.

1. Bridges to the π Cloud. The indole$-(water)_2$ cluster provides a first example of a water bridge structure, here stretched between the indole NH and π clouds. Figure 7a) shows the RIDIR spectrum of indole$-(water)_2$, compared to the calculated spectrum (Figure 7b) due to the lowest-energy structure, which contains the water bridge.[53,54] The infrared spectrum shows that the primary attachment of the water dimer to indole is via the indole NH group, as anticipated, based on the structure of the indole$-(water)_1$ complex (section V.B). The bridge fundamentals appear at 3488 and 3402 cm^{-1}, and are mixed NH/OH vibrations of the XH groups in the bridge. In addition, the spectrum shows clear evidence that the second water molecule does interact with the indole π cloud, producing OH stretch infrared transitions shifted down by -73 and -48 cm^{-1}, respectively, from the symmetric and antisymmetric stretches in the free water molecule, indicative of a π H-bond

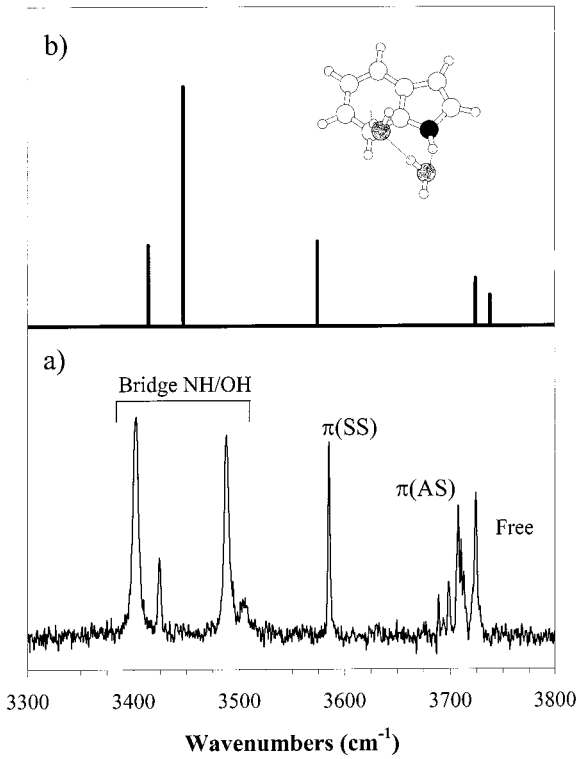

Figure 7. (a) Experimental RIDIR spectrum of the indole$-(H_2O)_2$ cluster. (b) Calculated harmonic vibrational frequencies and infrared intensities for the lowest-energy structure of indole$-(H_2O)_2$, shown as an inset. The calculations were carried out at the DFT Becke3LYP/6-31+G* level of theory. Harmonic frequencies were scaled by 0.9775.

comparable to that in benzene$-(H_2O)_2$.[69] The interaction with the indole π cloud is sufficient to bend the water dimer back over the indole ring, demonstrating the extraordinary flexibility of the water dimer bridge. Apparently, the strain energy induced by bridge formation in the NH···OH and OH···OH H-bonds is compensated for in forming the π H-bond and in cooperatively strengthening the bridge H-bonds. The formation of a water bridge despite the tenuous nature of the terminating π H-bond provides first evidence that water bridges may be a preferred structural motif in cases where it can be formed.

2. Bridges Involving Ket-Enol Tautomers. The keto−enol tautomers 2-pyridone (2PYR) and 2-hydroxypyridine (2HP) have adjacent H-bond donor and acceptor sites whose close proximity facilitates the formation of water bridges between them. The tautomers are virtually isoenergetic,[70] so that both

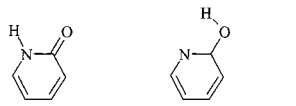

are present in substantial proportions in the expansion, enabling their study. 2-Pyridone is a constrained *cis*-amide with the same H-bonding sites as uracil. The 2PYR$-$(water)$_n$ clusters with $n = 1$ and 2 are known from the high-resolution ultraviolet spectroscopy of Held and Pratt to be bridge structures in which the water molecules accept a H-bond from the N−H group and donate to the carbonyl of 2PYR.[71] The RIDIR spectra of the 2PYR$-(H_2O)_{1,2}$ clusters are shown in Figure 8b,d, respectively.[72,73] The corresponding spectra of the 2HP$-(H_2O)_n$ clusters with $n = 1,2$ (Figure 8a,c) confirm that they also are bridge structures, this time with water spanning the gap between the pyridine nitrogen and OH groups.[73] As Figure 8 shows, the corresponding scans of 2HP$-(H_2O)_n$ and 2PYR$-(H_2O)_n$ are remarkably similar. While termination sites for the bridges are different in the two molecules, the total binding energies, the distance between these sites, and their relative orientation are similar enough that the bridge fundamentals mimic one another in the two circumstances.

The bridge fundamentals in Figure 8 appear between 3100 and 3400 cm^{-1}, shifted significantly further down in frequency than in indole$-(H_2O)_2$. They are also unusually broad, with widths nearly five times greater than that from other solute$-(H_2O)_2$ clusters that cannot form bridges. Both features are consistent with a strongly linked bridge with termination sites that can form strong H-bonds, spaced at a distance that is spanned well by two water molecules. The water−water separation in both the $n = 2$ bridges is unusually short, about 0.25 Å shorter than in the free water dimer.[71]

3. Other cis-Amide Bridges. The large frequency shifts and unusual widths of the bridge fundamentals appear to be quite general features of *cis*-amide$-$(water)$_n$ bridges. For instance, the water bridge structures produced by the constrained *cis*-amides oxindole (hereafter OI) and 3,4-dihydro-2(1H)-quinolinone (hereafter DQ) have bridge fundamentals with a very similar appearance.[74] In OI, the separation between the hydrogen and oxygen of the *cis*-amide group (2.63 Å) is about 0.2 Å larger than in the six-membered rings 2PYR and DQ (2.45 Å). The water bridges appear to be capable of adjusting to structural differences of this magnitude easily, showing little difference in the spectra of the water-containing clusters of the three molecules.

4. Ammonia-Containing Bridges. While water is arguably the most important solvent capable of forming H-bonded networks and bridges, other molecules can also serve this purpose. Ammonia is a prototypical base, which in most circumstances serves solely as a H-bond acceptor. For instance, only the HOH···NH_3 structure has been observed for the water−ammonia complex.[75,76] However, ammonia can be forced into circumstances where it acts both as H-bond acceptor and donor when it forms a H-bonded bridge, as it does in its interactions with *cis*-amides.

We have recently studied the infrared spectroscopy of a series of ammonia-containing clusters with OI and DQ,[77] all of which have the ammonia molecules involved in H-bonded bridges. The ammonia molecules in OI$-(NH_3)_{1,2}$ and DQ$-(NH_3)_{1,2}$ act as donors either to the carbonyl oxygen of the *cis*-amide, or to another ammonia molecule. Interestingly, two isomers each of OI$-(NH_3)-(H_2O)$ and DQ$-(NH_3)-(H_2O)$ are observed. The RIDIR spectra of these mixed NH_3/H_2O clusters prove that these two isomers differ in the ordering of the ammonia and water molecules in the bridge, as shown in Figure 9. Note that in isomer I, the ammonia molecule acts as donor to water rather than vica versa, despite the fact that such a bonding arrangement is never observed in the absence of the *cis*-amide template. The two isomers have similar binding energies for different reasons. Both isomers have one strong H-bond, one weak H-bond, and one H-bond of intermediate strength.

The effects of H-bond donation on the NH stretch vibrations of ammonia are seen clearly in the RIDIR spectrum of the OI−

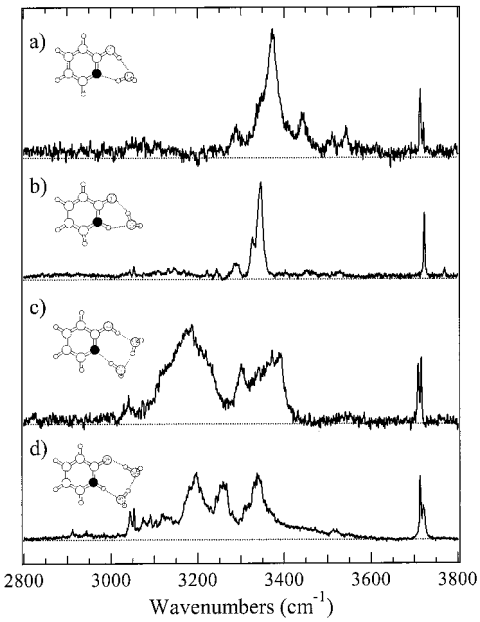

Figure 8. RIDIR spectra of (a) 2-hydroxypyridine$-(H_2O)_1$, (b) 2-pyridone$-(H_2O)_1$, (c) 2-hydroxypyridine$-(H_2O)_2$, and (d) 2-pyridone$-(H_2O)_2$.

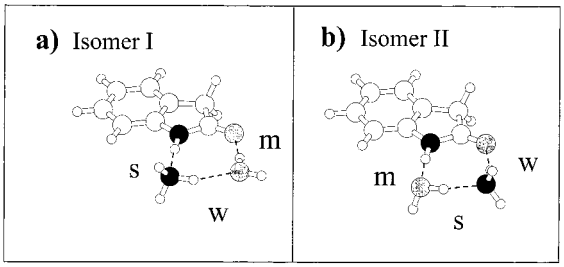

Figure 9. Calculated structures of the two experimentally observed structures of oxindole$-(H_2O)-(NH_3)$ complex. Note the changed order of the ammonia and water molecules in the bridge in the two isomers. The s, m, and w designations denote the relative strengths of the hydrogen bonds: s = strong, m = medium, and w = weak.

$(NH_3)_1$ complex (Figure 10a) and its comparison with calculation (Figure 10b). In the NH_3 monomer, the three NH bonds are equivalent, producing a totally symmetric NH stretch fundamental (a_1 symmetry in C_{3v}) at 3336 cm^{-1}, and a doubly degenerate "antisymmetric" stretch fundamental (e symmetry) at 3444 cm^{-1}.[78] When one of the NH bonds is involved in a H-bond as donor, the 3-fold symmetry of the NH bonds is broken. The doubly degenerate stretch is thereby split by an amount that correlates with the strength of the H-bond. The highest frequency mode is a free NH stretch, which is essentially unchanged in frequency and intensity from the ammonia monomer. The other two vibrations involve substantial motion of the H-bonded NH group. Both these latter vibrations are lowered in frequency by an amount that reflects the strength of the H-bond involved. They also gain almost a factor of 10 in intensity upon H-bond formation. These are the usual signatures of an XH group acting as a H-bond donor. The relative intensities of the two H-bonded NH stretch modes reflect the percent H-bonded NH stretch character in these modes. A simple reduced-dimension model of the NH stretch modes involving only the NH bonds is able to reproduce the experimental frequencies and intensities of the ammonia NH stretches in OI$-(NH_3)_1$, OI$-(NH_3)_2$, and two conformers of OI$-(NH_3)_1(H_2O)_1$.[77]

5. Water Bridges across the Carboxylic Acid Group. 3-Indolepropionic acid (IPA) has a carboxylic acid group with donor

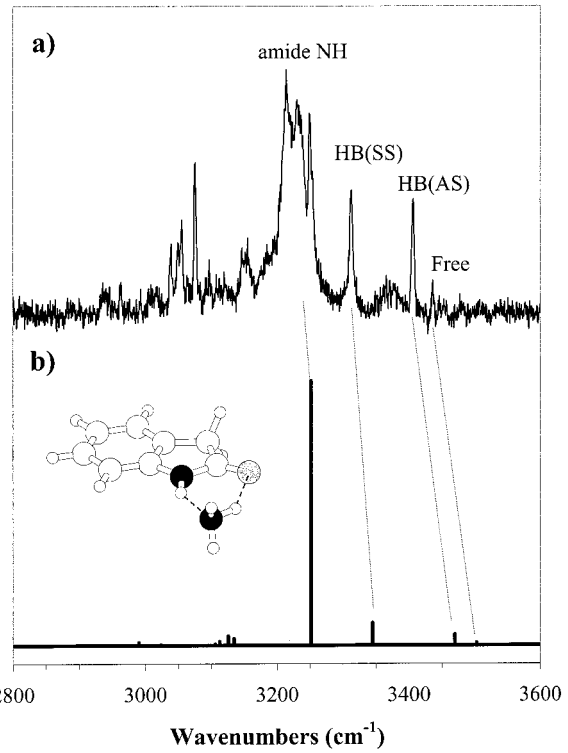

Figure 10. (a) RIDIR spectrum of the oxindole-NH_3 complex. (b) Calculated scaled harmonic vibrational frequencies and infrared intensities of the minimum-energy structure, shown as an inset. The three NH stretch modes of the ammonia molecule are labeled free, HB(AS), and HB(SS). See the text and ref 77 for further discussion.

OH and acceptor C═O groups adjacent to one another. As with the *cis*-amides just discussed, the close proximity of these groups enables even a single water molecule to bridge between these sites, forming a complex with a calculated total binding energy (9.1 kcal/mol after zero-point energy correction) that reflects the formation of two rather than a single H-bond. IPA is a flexible molecule whose conformational preferences have been considered already in section IV. In section VI, the effects of water bridges on the conformational preferences of flexible molecules will be discussed, including IPA. In this section attention is focused on the infrared spectroscopy of the H-bonded bridges themselves that here span the carboxylic acid group.

The RIDIR spectra of the dominant conformers of IPA$-(H_2O)_1$ and IPA$-(H_2O)_2$ are shown in Figure 11a,c, respectively.[79] As with the *cis*-amide$-(H_2O)_n$ bridges, the bridge fundamentals show striking broadening that distinguishes them at a glance from the water free OH and indole NH stretch fundamentals. The calculated spectra of IPA$-(H_2O)_{1,2}$ are shown below the experimental spectra in Figure 11b,d, with their bridge structures shown as insets. In both clusters, the lowest frequency OH stretch is largely localized on the carboxylic acid OH. The magnitude of its shift from the monomer frequency (3580 cm^{-1}) is large: −293 cm^{-1} in IPA$-W_1$ and −546 cm^{-1} in IPA$-W_2$. These large frequency shifts are consistent with this OH group being acidic. In addition, the formation of a water bridge produces cooperative strengthening of this H-bond. The calculated structure of IPA$-(H_2O)_2$ reflects this strengthening in a short water−water separation of 2.71 Å, almost 0.25 Å less than in the free water dimer, and comparable to that in the cis-amide$-(H_2O)_2$ clusters. At the same time, the water bridge OH stretch fundamentals of IPA$-(H_2O)_{1,2}$ are about 40−150 cm^{-1} above the corresponding band(s) in the *cis*-amide$-(H_2O)_{1,2}$ bridge complexes. Thus, the strong binding at the carboxylic acid OH group is maintained somewhat at the

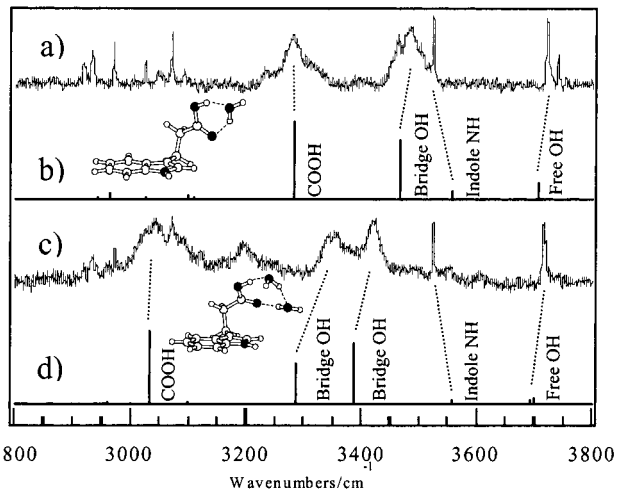

Figure 11. Experimental RIDIR spectra of (a) conformer A of IPA-H_2O and (c) conformer A of IPA$-(H_2O)_2$. Calculated scaled harmonic vibrational frequencies and infrared intensities for the Gpy(d) structures shown as insets in the figure. The absorption at 3200 cm^{-1} in (c) is attributed to the water bend overtone.

expense of a weaker interaction of the water dimer with the carboxylic acid C═O group.

6. Effect of Electronic Excitation on Water Bridges. Our chemical intuition about the strengths of hydrogen bonds is based almost entirely on the ground-state properties of the molecules involved. However, electronic excitation can produce dramatic changes in the H-bonding properties of a solute, strengthening some H-bonds and weakening others. In the most striking cases, electronic excitation can lead to excited-state proton transfer between solute and solvent.[32,80] However, even when this does not occur, the change in H-bonding environment can change the hydride stretch region of the infrared significantly, providing evidence for the effects of electronic excitation both on the solute itself and on the surrounding solvent. The challenge, of course, is to measure these changes. As noted in section III, S_1-state FDIR spectroscopy provides a means of recording the hydride stretch infrared spectrum of individual excited-state vibronic levels of a given sized cluster, free from interference from other species present in the expansion. When the ground-state structure is a water bridge, the S_1-state FDIR spectrum probes the effects of electronic excitation on the bridge. The hydrogen bonded bridges in the 2PYR$-(H_2O)_n$ clusters serve as a good illustration of this fact.

Parts a and b of Figure 12 show the FDIR spectra out of the S_1-state zero-point levels of 2PYR$-(H_2O)_n$ with $n = 1$ and 2, respectively. The spectrum in Figure 12a is essentially identical to that from Matsuda et al.,[81] while the spectrum of 2PYR$-(H_2O)_2$ (Figure 12b) has not been reported previously. The spectra in S_1 are to be compared with the corresponding spectra in the ground state, shown in Figure 8b,d, respectively. Recall that the two bridge fundamentals in S_0 2PYR$-(H_2O)_1$ are near-equal mixes of *cis*-amide NH and water OH groups, largely canceling the intensity of the lower frequency fundamental in which the bridge NH and OH groups oscillate in phase with one another.[73] In S_1, both bridge fundamentals carry substantial intensity, and the lower frequency transition is largely NH stretch in character. Its frequency is similar in the two electronic states. However, the water OH stretch is almost 150 cm^{-1} higher in frequency in S_1 than in S_0. Matsuda et al.[81] concluded on this basis that the amide NH H-bond is hardly changed in strength by electronic excitation, while the HOH···O═C H-bond is weakened significantly. This is the same qualitative result as

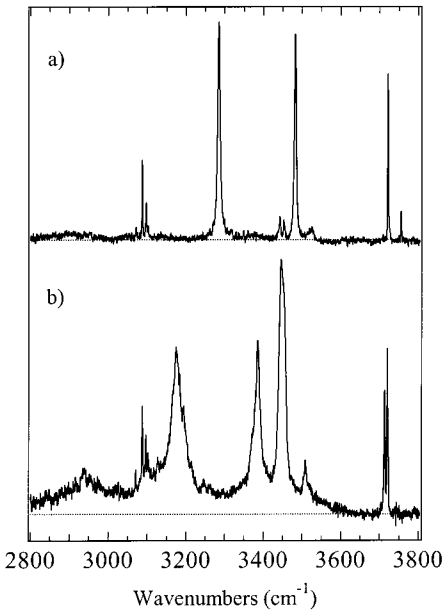

Figure 12. S_1-state FDIR spectra of the (a) 2-pyridone$-(H_2O)_1$ and (b) 2-pyridone$-(H_2O)_2$ complexes. Compare these to the corresponding spectra in the ground electronic state (Figure 8) to see the effects of electronic excitation on the water bridge.

found in the mixed 2PYR-2HP dimer, which reorients upon electronic excitation in such a way as to increase the OH···O═C H-bond distance, thereby raising the frequency of this OH stretch fundamental by several hundred wavenumbers.[82] One can surmise on this basis that the carbonyl group of 2-pyridone is not as good a H-bond acceptor in the excited state as in the ground state, while the NH group is a comparable donor. The effect of electronic excitation on the vibrational modes is also significant, because the coupling of the oscillators along the bridge is thereby removed. This lack of coupling is also reflected in the narrower widths of the bridge fundamentals in S_1 relative to S_0.

The corresponding spectrum of 2PYR$-(H_2O)_2$ (Figure 12b) leads to similar conclusions. The cis-amide NH stretch is hardly changed upon electronic excitation, but the two water bridge OH stretch fundamentals are 100−150 cm^{-1} above their frequency in the ground-state spectrum (Figure 8d), indicating a substantial weakening of the both the water−water and water−carbonyl H-bonds. This decouples the vibration of the NH bond from the two water OH groups in the bridge.

VI. Influence of Water Bridges on the Conformational Preferences of Flexible Biomolecules

In section IV, experiments were described that determine the infrared and ultraviolet spectra of single conformations of flexible molecules. Two tryptophan analogues, tryptamine and 3-indole-propionic acid, have played starring roles in these discussions. Here we use these same two molecules as templates for forming water-containing clusters.[79] Elements of this story have already been discussed in section IV, but the issue of the influence of water solvation, particularly in the form of water bridges, on the conformational preferences of these molecules is addressed here.

The reader will recall that the IPA monomer has two conformations with significant population in the expansion: one with the carboxylic acid in the gauche position on the pyrrole side of indole (Gpy), the other in the anti position (Figure 4). The R2PI spectra of the IPA$-(H_2O)_1^+$ and IPA$-(H_2O)_2^+$ mass

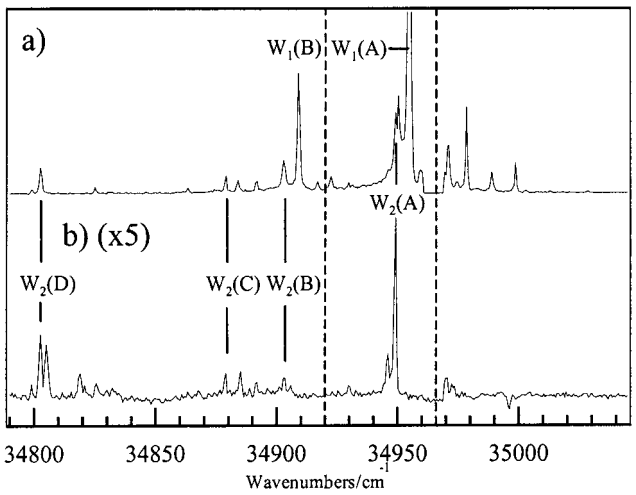

Figure 13. R2PI spectra of IPA$-(H_2O)_n^+$ mass channels with (a) $n =$ 1 and (b) $n = 2$. The label W_n(A) designates conformer A of IPA$-(H_2O)_n$. The transitions due to IPA-W_2 appear in both mass channels due to fragmentation following photoionization. Dashed lines represent the IPA monomer A and B origins at 34966 and 34920 cm^{-1}, respectively.

channels is shown in Figure 13a,b, respectively. Interestingly, while there are two conformers of IPA$-(H_2O)_1$, there are four conformers of IPA$-(H_2O)_2$. The comparison of the R2PI with that of the IPA monomer (Figure 4b) shows that the two transitions assigned to IPA$-(H_2O)_1$ and the two most intense transitions assigned to IPA$-(H_2O)_2$ (designated as $W_{1,2}$(A,B) in the figure) show only small changes in frequency from the IPA(A = Gpy) and IPA(B = anti) monomer transitions. The A/B pairs also share similar relative intensities with the corresponding A/B monomer transitions, suggesting that the clusters responsible for these transitions retain the conformational preferences of the IPA monomer, with the COOH group in the gauche pyrrole position in $W_{1,2}$(A) and in the anti position in $W_{1,2}$(B), as deduced by Connell et al.[83] on the basis of their rotational coherence measurements. At the same time, the RIDIR spectra of Figure 11a,c show clearly that the water molecule(s) in these complexes form bridges between the carbonyl and OH groups of the carboxylic acid. Thus, the water bridges formed in IPA(A,B)$-(H_2O)_{1,2}$ bind to IPA in such a way that the conformational preferences of the IPA monomer are unchanged.

However, the W_2(C) and W_2(D) R2PI transitions in Figure 13 are without analogues in the IPA monomer and have not been observed in previous work.[55,83] These R2PI transitions are shifted further to the red than W_2(A) and W_2(B), indicating a stronger interaction with indole's π cloud. Their RIDIR spectra are shown in Figure 14a) and 14b). A striking feature of these spectra is the π H-bonded OH stretch bands that appear in both spectra in the 3650−3670 cm^{-1} region characteristic of the weak H-bond formed between a water OH and the indole π cloud.[54] Apart from this, the spectra are reminiscent of the W_2(A) bridge structure (Figure 11b). The π H-bonded OH stretch can only occur if the COOH group is in the gauche-phenyl position, as shown in the inset of Figure 14c. Low-lying minima of this type have been identified via the DFT calculations. The calculated hydride stretch IR spectra of these structures (e.g., Figure 14c) correctly predict the presence of a π H-bond, confirming the structural identification. Thus, in the IPA$-(H_2O)_2$ clusters, the formation of water dimer bridges across the carboxylic acid group produces and stabilizes population in the gauche-phenyl conformation even though this conformation is not represented significantly in the IPA monomer population due to its higher energy.

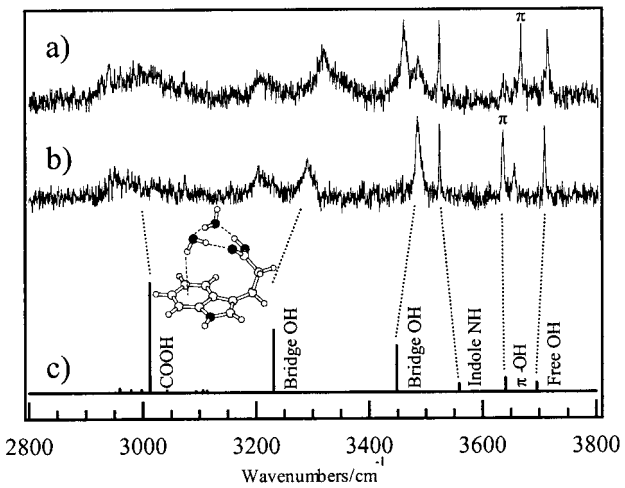

Figure 14. Experimental RIDIR spectra of (a) IPA(C)$-(H_2O)_2$ and (b) IPA(D)$-(H_2O)_2$. (c) Calculated IR spectrum of one of the gauche-phenyl IPA$-(H_2O)_2$ minima (shown as an inset). The absorption at 3200 cm^{-1} in (a,b) is attributed to the water bend overtone.

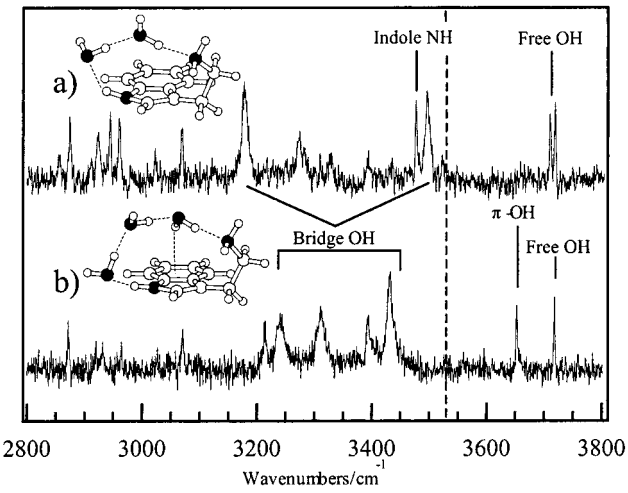

Figure 15. Experimental RIDIR spectra of (a) TRA$-(H_2O)_2$ and (b) TRA$-(H_2O)_3$. Calculated structures for TRA$-(H_2O)_2$ and TRA$-(H_2O)_3$ that are consistent with the experimental spectra are shown as insets. The position of the free indole-NH is marked with a dashed line at 3525 cm^{-1}.

In TRA$-(H_2O)_2$ and TRA$-(H_2O)_3$, water bridges are also formed, but here they stretch between the amino acceptor and the indole NH donor sites.[79] The reader will recall that the first water molecule attaches to TRA preferentially at the amino group, but cannot reach to the indole NH (Figure 6b). Nevertheless, the seven conformations with population in the TRA monomer are collapsed into a single dominant conformation upon this binding (Gpy(out)).[47,55] The RIDIR spectrum of the TRA$-(H_2O)_2$ (Figure 15a) shows the two bridge OH stretch fundamentals anticipated for a water dimer attached to the amino group, and an indole NH stretch that is shifted slightly down in frequency by −48 cm^{-1} from its value in the monomer, indicating that one of the water molecules is interacting weakly with the indole NH.

Similarly, in TRA$-(H_2O)_3$, the RIDIR spectrum (Figure 15b) shows a set of bridge hydride stretch fundamentals in the 3200−3450 cm^{-1} region assignable to the indole NH and three water OH groups making up the bridge. One of the free OH groups is now involved in a π H-bond with the indole ring. Extensive searches for cluster structures consistent with these features have been carried out. Calculated TRA$-(H_2O)_2$ and TRA$-(H_2O)_3$

structures consistent with the RIDIR spectra are shown as insets in Figure 15. Notably, in both TRA−$(H_2O)_2$ and TRA−$(H_2O)_3$, formation of the water bridge can only be accomplished at an amino orientation that points the amino group's lone pair in toward the indole π cloud. This conformation is nominally one of the two highest-energy conformations from Figure 1, which is not observed in the TRA monomer spectrum because of the destabilization associated with the nitrogen lone pair pointing in toward the indole π cloud.[10,11] However, the added stabilization achieved by forming the water bridge far exceeds the inherent strain of the ethylamine side chain in this orientation.

It is worth considering yet how these conformations come to be populated in the clusters. Clearly, the form of the potential energy surface along the intramolecular internal coordinates will change in the presence of water bound to various sites. However, the surprising fact is that the propionic acid or ethylamine conformations taken up by IPA and TRA in the water-containing clusters are ones without significant monomer population in the expansion. One might have anticipated that the distribution of monomer conformations would dictate the conformations taken up by the water-containing clusters, but this is clearly not so.

Instead, the results on TRA−$(H_2O)_n$ and IPA−$(H_2O)_n$ clusters indicate that the new conformations must be populated and stabilized in the process of forming the H-bond(s) with water. The energy released by H-bond formation to the monomer gives energy to the flexible sites in the monomer to overcome the barriers separating minima, effectively annealing the molecule into new conformations not accessible to the bare molecule at the preexpansion temperature (T∼410 K). Subsequent cooling in the expansion then traps the cluster in these new conformations. In IPA−$(H_2O)_2$, this was a minor route forming the gauche phenyl conformation, which expanded the number of conformations observed. In TRA−$(H_2O)_n$, the seven monomer conformations are reduced in number by water complexation.

In either case, when water bridge formation can occur, it appears to be a preferred structural motif from an energetic standpoint, even if formation of the bridge necessitates a substantial reconfiguration of the monomer away from its preferred conformation(s) in the absence of the bridge. From a practical standpoint, these results indicate that it would be misguided to consider only the lowest-lying monomer conformations (i.e., those with population in the expansion) as starting geometries for geometry optimizations of water-containing clusters of flexible molecules.

It is worth considering whether water molecules might play a similar role in inducing conformational change via H-bond formation and breakup in room-temperature aqueous solution. One typically thinks of conformational changes occurring in solution as occurring by random, statistical fluctuations in a molecule's energy due to collisions with the surrounding solvent. However, a molecular-scale view of such processes would suggest that the formation of critical solute−solvent structures, such as water bridges, might be the means by which extra energy could be released into the solute at the bridge termination sites, thereby inducing conformational change that could be stabilized upon breakup of the bridge.

VII. Future Prospects

This review has touched on several issues of importance to the broader field of the spectroscopy of gas-phase biomolecules. This field is undergoing explosive growth due to a synergism between the ever-improving experimental methodologies on one hand and computational capabilities on the other. Several groups have demonstrated the ability to put complex, biologically relevant molecules into the gas phase, cool them in a supersonic expansion, and probe them subsequently either as bare molecules or as clusters with water or other common solvents, using a range of laser-based spectroscopy methods.[18,84−88] State-of-the-art ab initio and density functional theory methods can then be used to distinguish between the possible structures and to test the molecular force fields in common usage.

A specific theme of the present review has been that of water bridges, a structure often taken up by water molecules attached to solutes with both hydrogen bond donor and acceptor sites. Resonant ion-dip infrared spectroscopy has provided infrared spectral signatures for these bridge structures as a function of cluster size and molecular conformation. The bridge fundamentals typically occur in the 3100−3400 cm^{-1} region, with frequencies, intensities, and widths that reflect the nature of the termination sites, their separation, their relative orientation, and the number of water molecules spanning them.

In looking to the future, several areas are in need of further exploration. The molecules studied to date by our group have had H-bond donor and acceptor sites at distances that could be spanned by water bridges containing no more than three water molecules. However, recent studies have shown that water bridges will be a recurring structural theme even when the H-bonding sites are even further separated from one another. For instance, *trans*-formanilide has a *trans*-amide group in which the N−H and C═O sites point in opposite directions. Yet, recent studies by Robertson[67] have shown that the *trans*-formanilide−$(H_2O)_4$ cluster contains a water bridge that spans these two "remote" sites. Similarly, Bach et al.[64−66] have reported water bridges of up to four water molecules spanning the distance between the OH group and nitrogen atoms of 7-hydroxyquinoline, while Mitsui et al.[31,89,90] have extended the bridge to five water molecules in joining the N−H and C═O sites on opposite sides of the aromatic rings in 9(10H)-acridone.

Bridges connecting a wider range of H-bond donor/acceptor combinations need yet to be studied. Such studies will naturally include molecules with more than two H-bonding sites, where the relative distance between these sites and the strength of the bridges that can be produced could lead to interesting changes in the preference for competing sites as a function of the number of water molecules in the cluster. It seems likely that branched bridges,[31] and other more exotic H-bonding networks will also be formed in some cases. The spectroscopic analysis of such systems will be a substantial challenge to both experiment and theory.

One can also change the solvent composition of the bridge. The mixed ammonia−water bridges in oxindole (section V.B.4) illustrate the counterbalancing forces that can lead to solvent bridges of varying solvent order and strikingly different spectral properties.

The spectra of water bridges also hold information yet to be extracted about the dynamics of the coupled oscillators in the bridge. Mode-specific broadening of the hydride stretch vibrations is readily apparent in most of the spectra reported in this article. The bridge fundamentals themselves are strikingly broadened relative to the hydride stretches not involved in the bridge (e.g., the free OH stretches). Quantitative accounts of these differences are still needed. Furthermore, the generality and importance of such broadening extends well beyond water-containing bridges. For instance, the amide NH stretch fundamentals of both oxindole−$(NH_3)_2$ and oxindole dimer are split by Fermi resonances extending over more than 300 cm^{-1}. Similar broadening and sub-structure is observed in other strongly H-bonded dimers including benzoic acid dimer,[91]

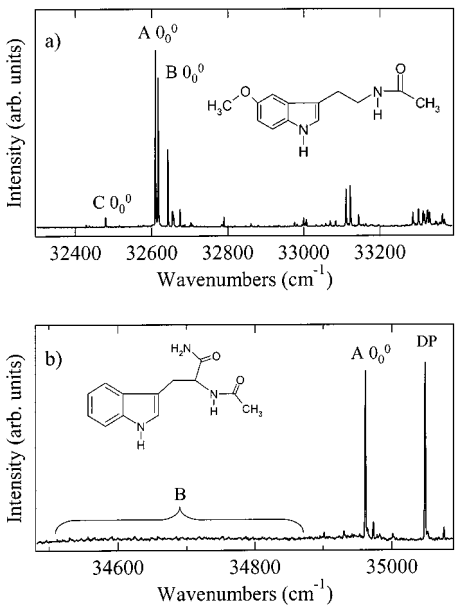

Figure 16. (a) Two-color R2PI spectrum of melatonin in the region of the S_1-S_0 origin. (b) Analogous LIF excitation scan of *N*-acetyl tryptophan amide (NATA) in the region of its S_1-S_0 origin. The transition marked "DP" is due to a thermal decomposition product.

pyridone dimer,[72,81] and the mixed 2-pyridone/2-hydroxypyridine dimer.[82]

Beyond the vibrational dynamics, water bridges are thought to play a potentially important role in proton-transfer reactions between remote acid and base sites in biological systems.[6,7] The study of proton transfer in well-characterized water bridge clusters should enable a clear analysis of the effects of the structural requirements, efficiency, and time scales of these processes as a function of cluster size. Leutwyler and co-workers have recently demonstrated the potential for such studies in their observation of size-dependent excited-state proton transfer in 7-hydroxyquinoline$-(NH_3)_n$ clusters.[32,80]

A second theme of this article has been the study of the spectroscopy of single conformations of flexible molecules. The ability of the double resonance methods to record the infrared and ultraviolet spectral signatures of individual conformations enables one to establish and then understand the conformational preferences of these molecules. The natural progression in this area will be toward monomers of ever-greater complexity and biological relevance. A necessary prerequisite for success in such studies will be the ability to entrain these larger molecules in the expansion in sufficient quantities for spectroscopic detection without decomposition. The recent successes of the de Vries group[92−94] using laser desorption sources to study the R2PI spectroscopy of dipeptides and nucleosides has confirmed the potential for fruitful spectroscopy with such sources.

However, beyond the question of whether one can produce sufficiently dense, jet-cooled beams of these molecules, one might wonder whether the shear number of conformational isomers might increase so quickly with molecule size that the spectroscopic analysis will quickly become unmanageable. While it is still too early to assess this point in a general way, there is growing evidence that the number of thermally accessible conformers does not increase exponentially with molecular size, but may in fact remain relatively constant, or even decrease. For example, Figure 16a shows the 2-color R2PI spectrum of melatonin,[95] while Figure 16b shows the LIF excitation spectrum of the dipeptide analogue *N*-acetyl tryptophan amide (NATA).[49] Both these molecules have several more flexible internal coordinates than either tryptamine or 3-indole-propionic acid. However, the spectrum of melatonin can be ascribed to only three conformations, while NATA's spectrum is dominated by a single conformation (A). While the minor conformer of NATA (labeled B in Figure 16b) has some very interesting spectroscopic properties, the main point here is that the spectra of NATA and melatonin do not show an exponentiation in the number of conformers observed, making it possible to obtain RIDIR and FDIR spectra of single conformations of these larger molecules.[49] Thus, the bulkier groups and the relative rigidity of the amide subunits place significant constraints that may limit the number of conformations observed even in larger polypeptides.

Once the spectroscopy and conformational preferences of the monomers are in hand, these larger molecules will be interesting candidates in which to assess the effects of water on their conformational preferences. As the size of the solute molecule grows, the potential for intramolecular hydrogen bonds also will increase. Complexation with water could lead to a competition between intramolecular and intermolecular hydrogen bonds, or to a strengthening of the intramolecular hydrogen bonds by water bridges. The influence of water solvation, and more particularly water bridge formation, on the conformational preferences of flexible monomers of ever greater complexity will be a fascinating and challenging arena in which to apply the methods highlighted in this article. They also will present a particular challenge to computational chemists, and those seeking to improve semiempirical force fields. Fast, accurate methods for screening the conformational possibilities, assessing the potential structures of the water-containing clusters, and calculating the infrared spectra are high priorities if the potential of this field is to be fully realized.

Acknowledgment. The author gratefully acknowledges the National Science Foundation Experimental Physical Chemistry Program for their support of this work (CHE9728636). Dr. Joel R. Carney, Dr. Christopher J. Gruenloh, Gina M. Florio, Brian C. Dian, Sebastien Mercier, Dr. Asier Longarte, Dr. Andrei Fedorov, and Prof. John Cable all contributed to the work reviewed here. The author thanks them for their hard work, enthusiasm, and scientific insight that has made day-to-day interactions with them such a joy.

References and Notes

(1) Marchi, M.; Borgis, D.; Levy, N.; Ballone, P. *J. Chem. Phys.* **2001**, *114*, 4377−4385.

(2) Kollman, P. A.; Massova, I.; Reyes, C.; Kuhn, B.; Huo, S. H.; Chong, L.; Lee, M.; Lee, T.; Duan, Y.; Wang, W.; Donini, O.; Cieplak, P.; Srinivasan, J.; Case, D. A.; Cheatham, T. E. *Acc. Chem. Res.* **2000**, *33*, 889−897.

(3) Cheatham, T. E.; Kollman, P. A. *Annu. Rev. Phys. Chem.* **2000**, *51*, 435−471.

(4) Fernandez-Ramos, A.; Smedarchina, Z.; Siebrand, W.; Zgierski, M. Z. *J. Chem. Phys.* **2000**, *113*, 9714−9721.

(5) Petukhov, M.; Cregut, D.; Soares, C. M.; Serrano, L. *Protein Sci.* **1999**, *8*, 1982−1989.

(6) Toba, S.; Colombo, G.; Merz, K. M. *J. Am. Chem. Soc.* **1999**, *121*, 2290−2302.

(7) Fedorov, A.; Shi, W.; Kicska, G.; Fedorov, E.; Tyler, P. C.; Furneaux, R. H.; Hanson, J. C.; Gainsford, G. J.; Larese, J. Z.; Schramm, W. L.; Almo, S. C. *Biochemistry* **2001**, *40*, 853−860.

(8) Sadeghi, R. R.; cheng, H. P. *J. Chem. Phys.* **1999**, *111*, 2086−2094.

(9) Fenn, J. B. *Annu. Rev. Phys. Chem.* **1996**, *47*, 1−41.

(10) Carney, J. R.; Zwier, T. S. *J. Phys. Chem. A* **2000**, *104*, 8677−8688.

(11) Carney, J. R.; Zwier, T. S. *Chem. Phys. Lett.* **2001**. In press.

(12) Ruoff, R. S.; Klots, T. D.; Emilsson, T.; Gutowsky, H. S. *J. Chem. Phys.* **1990**, *93*, 3142−3150.

(13) Zwier, T. S. *Annu. Rev. Phys. Chem.* **1996**, *47*, 205−241.

(14) Connell, L. L.; Corcoran, T. C.; Joireman, P. W.; Felker, P. M. *J. Phys. Chem.* **1990**, *94*, 1229−1232.
(15) Dian, B. C.; Zwier, T. S. Unpublished results.
(16) Fraser, G. T.; Suenram, R. D.; Lugez, C. L. *J. Phys. Chem. A* **2000**, *104*, 1141−1146.
(17) Keske, J.; McWhorter, D. A.; Pate, B. H. *Int. Rev. Phys. Chem.* **2000**, *19*, 363−407.
(18) Rizzo, T. R.; Park, Y. D.; Peteanu, L. A.; Levy, D. H. *J. Chem. Phys.* **1986**, *84*, 2534−41.
(19) Philips, L. A.; Levy, D. H. *J. Chem. Phys.* **1988**, *89*, 85−90.
(20) Felker, P. M. *J. Phys. Chem.* **1992**, *96*, 7844.
(21) Felker, P. M. *Chem. Rev.* **1994**, *94*, 1784.
(22) Liu, K.; Cruzan, J. D.; Saykally, R. J. *Science* **1995**, *271*, 929−33.
(23) Pratt, D. W. *Annu. Rev. Phys. Chem.* **1998**, *49*, 481−530.
(24) Provencal, R. A.; Paul, J. B.; Chapo, C. N.; Saykally, R. J. *Spectroscopy* **1999**, *14*, 24.
(25) Buck, U.; Ettischer, I.; Melzer, M.; Buch, V.; Sadlej, J. *Phys. Rev. Lett.* **1998**, *80*, 2578.
(26) Riehn, C.; Lahmann, C.; Wassermann, B.; Brutschy, B. *Ber. Bunsen-Ges. Phys. Chem.* **1992**, *96*, 1161−64.
(27) Ebata, T.; Fujii, A.; Mikami, N. *Int. Rev. Phys. Chem.* **1998**, *17*, 331−362.
(28) Robertson, E. G.; Simons, J. P. *Phys. Chem. Chem. Phys.* **2001**, *3*, 1−18.
(29) Janzen, C.; Spangenberg, D.; Roth, W.; Kleinermanns, K. *J. Chem. Phys.* **1999**, *110*, 9898−9907.
(30) Brutschy, B. *Chem. Rev.* **2000**, *100*, 3891−3920.
(31) Mitsui, M.; Ohshima, Y.; Isiuchi, S.-i.; Sakai, M.; Fujii, M. *J. Phys. Chem. A* **2000**, *104*, 8649−8659.
(32) Coussan, S.; Meuwly, M.; Leutwyler, S. *J. Chem. Phys.* **2001**, *114*, 3524−3534.
(33) Kinsey, J. L. *Annu. Rev. Phys. Chem.* **1977**, *28*, 349.
(34) Johnson, P. M.; Berman, M. R.; Zakheim, D. *J. Chem. Phys.* **1975**, *62*, 2500.
(35) Boesl, U.; Neusser, H. J.; Schlag, E. W. *J. Chem. Phys.* **1980**, *72*, 4327−4333.
(36) Dietz, T. G.; Duncan, M. A.; Liverman, M. G.; Smalley, R. E. *J. Chem. Phys.* **1980**, *73*, 4816−4821.
(37) Murakami, J.-i.; Kaya, K.; Ito, M. *J. Chem. Phys.* **1980**, *72*, 3263−3270.
(38) Bach, A.; Coussan, S.; Muller, A.; Leutwyler, S. *J. Chem. Phys.* **2000**, *112*, 1192−1203.
(39) Pimentel, G. C.; McClellan, A. L. *The Hydrogen Bond*; W. H. Freeman: San Francisco, 1960.
(40) Page, R. H.; Shen, Y. R.; Lee, Y. T. *J. Chem. Phys.* **1988**, *88*, 5362−76.
(41) Page, R. H.; Shen, Y. R.; Lee, Y. T. *J. Chem. Phys.* **1988**, *88*, 4621−4636.
(42) Walther, T.; Bitto, H.; Minton, T. K.; Huber, J. R. *Chem. Phys. Lett.* **1994**, *231*, 64−69.
(43) Devlin, J. P.; Sadlej, J.; Buch, V. *J. Phys. Chem. A* **2001**, *105*, 974−983.
(44) Friesner, R. A.; Murphy, R. B.; Beachy, M. D.; Ringnalda, M. N.; Pollard, W. T.; Dunietz, B. D.; Cao, Y. X. *J. Phys. Chem. A* **1999**, *103*, 1913−1928.
(45) Park, Y. D.; Rizzo, T. R.; Peteanu, L. A.; Levy, D. H. *J. Chem. Phys.* **1986**, *84*, 6539−49.
(46) Wu, Y. R.; Levy, D. H. *J. Chem. Phys.* **1989**, *91*, 5278−5284.
(47) Connell, L. L.; Corcoran, T. C.; Joireman, P. W.; Felker, P. M. *Chem. Phys. Lett.* **1990**, *166*, 510−516.
(48) Snoek, L. C.; Robertson, E. G.; Kroemer, R. T.; Simons, J. P. *Chem. Phys. Lett.* **2000**, *321*, 49−56.
(49) Dian, B. C.; Longarte-Aldamo, A.; Mercier, S.; Zwier, T. S. Unpublished results.
(50) Korter, T. M.; Pratt, D. W.; Kupper, J. *J. Phys. Chem. A* **1998**, *102*, 7211−7216.
(51) Neusser, H. J.; Siglow, K. *Chem. Rev.* **2000**, *100*, 3921−3942.
(52) Mons, M.; Dimicoli, I.; Tardivel, B.; Piuzzi, F.; Brenner, V.; Millie, P. *J. Phys. Chem. A* **1099**, *103*, 9958−9965.
(53) Carney, J. R.; Hagemeister, F. C.; Zwier, T. S. *J. Chem. Phys.* **1998**, *108*, 3379−3382.
(54) Carney, J. R.; Zwier, T. S. *J. Phys. Chem. A* **1999**, *103*, 9943−9957.
(55) Peteanu, L. A.; Levy, D. H. *J. Phys. Chem.* **1988**, *92*, 6554−61.
(56) Huang, Y.; Sulkes, M. *J. Phys. Chem.* **1996**, *100*, 16749−16486.
(57) Frost, R. K.; Hagemeister, F. C.; Arrington, C. A.; Schleppenbach, D.; Zwier, T. S.; Jordan, K. D. *J. Chem. Phys.* **1996**, *105*, 2605−17.
(58) Sekiya, H.; Hamabe, H.; Ujita, H.; Nakano, N.; Nishimura, Y. *Chem. Phys. Lett.* **1996**, *255*, 437−444.
(59) Dickinson, J. A.; Hockridge, M. R.; Robertson, E. G.; Simons, J. P. *J. Phys. Chem. A* **1999**, *103*, 6938−6949.
(60) Dickinson, J. A.; Hockridge, M. R.; Robertson, E. G.; Simons, J. P. *J. Phys. Chem. A* **1999**, *103*, 6938−6949.
(61) Fedorov, A. V.; Cable, J. R. *J. Phys. Chem. A* **2000**, *104*, 4943−4952.
(62) Mons, M.; Dimicoli, I.; Tardivel, B.; Piuzzi, F.; Robertson, E. G.; Simons, J. P. *J. Phys. Chem. A* **2001**, *105*, 969−973.
(63) Carney, J. R.; Zwier, T. S.; Fedorov, A.; Cable, J. R. Unpublished results.
(64) Bach, A.; Coussan, S.; Muller, A.; Leutwyler, S. *J. Chem. Phys.* **2000**, *113*, 9032−9043.
(65) Bach, A.; Leutwyler, S. *Chem. Phys. Lett.* **1999**, *299*, 381−388.
(66) Bach, A.; Coussan, S.; Muller, A.; Leutwyler, S. *J. Chem. Phys.* **2000**, *112*, 1192−1203.
(67) Robertson, E. G. *Chem. Phys. Lett.* **2000**, *325*, 299−307.
(68) Xantheas, S. S. *J. Chem. Phys.* **1994**, *100*, 7523.
(69) Fredericks, S.; Jordan, K. D.; Zwier, T. S. *J. Phys. Chem.* **1996**, *100*, 7810−7821.
(70) Hatherley, L. D.; Brown, R. D.; Godfrey, P. D.; Pierlot, A. P.; Caminati, W.; Damiani, D.; Melandri, S.; Favero, L. B. *J. Phys. Chem.* **1993**, *97*, 46−51.
(71) Held, A.; Pratt, D. W. *J. Am. Chem. Soc.* **1993**, *115*, 9708−17.
(72) Matsuda, Y.; Ebata, T.; Mikami, N. *J. Chem. Phys.* **1999**, *110*, 8397−8407.
(73) Florio, G. M.; Gruenloh, C. J.; Quimpo, R. C.; Zwier, T. S. *J. Chem. Phys.* **2000**, *113*, 11143−11153.
(74) Carney, J. R.; Zwier, T. S.; Fedorov, A. V.; Cable, J. R. *J. Phys. Chem. A* **2001**, *105*, 3487−3497.
(75) Engdahl, A.; Nelander, B. *J. Chem. Phys.* **1989**, *91*, 6604−6612.
(76) Stockman, P. A.; Bumgarner, R. E.; Suzuki, S.; Blake, G. A. *J. Chem. Phys.* **1992**, *96*, 2496−2510.
(77) Fedorov, A.; Carney, J. R.; Cable, J. R.; Zwier, T. S. *J. Phys. Chem. A* In press.
(78) Guelachvili, G.; Abdullah, A. H.; Tu, N.; Rao, K. N.; Urban, S. *J. Mol. Spectrosc.* **1989**, *133*, 345.
(79) Carney, J. R.; Dian, B. C.; Florio, G. M.; Zwier, T. S. *J. Am. Chem. Soc.* **2001**, *123*, 5596−5597.
(80) Bach, A.; Leutwyler, S. *J. Chem. Phys.* **2000**, *112*, 560−565.
(81) Matsuda, Y.; Ebata, T.; Mikami, N. *J. Chem. Phys.* **2000**, *113*, 573−580.
(82) Borst, D. R.; Florio, G. M.; Muller, A.; Pratt, D. W.; Zwier, T. S.; Leutwyler, S. In preparation.
(83) Connell, L. L. Structural Studies of Hydrogen-bonded Clusters using Rotational Coherence Spectroscopy. University of California at Los Angeles, 1991.
(84) Cable, J. R.; Tubergen, M. J.; Levy, D. H. *J. Am. Chem. Soc.* **1988**, *110*, 7349−55.
(85) Li, L.; Lubman, D. M. *Rev. Sci. Instrum.* **1988**, *59*, 557.
(86) Meijer, G.; de Vries, M. S.; Hunziker, H. E.; Wendt, H. R. *Appl. Phys. B* **1990**, *51*, 395−403.
(87) Piuzzi, F.; Dimicoli, I.; Mons, M.; Tardivel, B.; Zhao, Q. *Chem. Phys. Lett.* **2000**, *320*, 282.
(88) de Vries, M. S. *Rev. Anal. Chem.* **2000**, *19*, 269−287.
(89) Mitsui, M.; Ohshima, Y. *J. Phys. Chem. A* **2000**, *104*, 8638−8648.
(90) Mitsui, M.; Ohshima, Y.; Kajimoto, O. *J. Phys. Chem. A* **2000**, *104*, 8660−8670.
(91) Florio, G. M.; Sibert, E. L., III; Zwier, T. S. *Faraday Discuss.* **2001**, *118*. In press.
(92) Nir, E.; Kleinermanns, K.; de Vries, M. S.; *Nature* **2000**, *408*, 949−951.
(93) Nir, E.; Imhof, P.; Kleinermanns, K.; de Vries, M. S.; *J. Am. Chem. Soc.* **2000**, *122*, 8091−8092.
(94) Cohen, R.; Brauer, B.; Nir, E.; Grace, L.; de Vries, M. S.; *J. Phys. Chem. A* **2000**, *104*, 6351−6355.
(95) Florio, G. M.; Zwier, T. S. In preparation.